Available online at www.eccomasproceedia.org
Eccomas Proceedia COMPDYN (2025) 707- 720

ECCOMAS
Proceedia

COMPDYN 2025
10th ECCOMAS Thematic Conference on
Computational Methods in Structural Dynamics and Earthquake Engineering
M. Papadrakakis, M. Fragiadakis (eds.)
Rhodes Island, Greece, 15-18 June 2025

SEISMIC RETROFIT OF RC BEAM-COLUMN JOINTS WITH EXTERNAL DISSIPATION DEVICES: A NUMERICAL STUDY

Paolo Ielpo[1,2], Giuseppe Santarsiero[2], Valentina Picciano[2] and Angelo Masi[2]

[1]Department of Earth and Geoenvironmental Sciences, University of Bari,
Via Orabona 4, 70125, Bari, Italy
e-mail: p.ielpo@phd.uniba.it

[2]Department of Engineering, University of Basilicata,
Via dell'Ateneo Lucano 10, 85100, Potenza, Italy
{paolo.ielpo, giuseppe.santarsiero, valentina.picciano, angelo.masi}@unibas.it

Abstract

The European building stock has a significant seismic vulnerability, largely due to designs that do not comply with current regulations. To mitigate this risk, effective and sustainable structural strengthening strategies are required. It is important to develop low-impact solutions to reduce costs and avoid interruptions to the building operation during strengthening interventions. In this context, the SPEAD technique (Steel Plate Energy Absorption Device) emerges as an innovative local strengthening device, offering a non-invasive solution to improve the flexural strength of reinforced concrete beams and columns. The SPEAD device allows for precise calibration of the strength increase, ensuring full compliance with capacity design criteria, thus optimizing the seismic behaviour of the structure. In addition, the local strengthening system is designed to effectively absorb seismic energy, dissipating it through steel hysteresis mechanisms. Thanks to its non-invasive nature, it can be applied without interrupting the use of the building (i.e. from the outside), ensuring operability for the end users. This study aims to develop an advanced numerical model to simulate the behaviour of beam-column joints subjected to seismic loading. By implementing a nonlinear 3D model, the goal is to accurately capture local damage mechanisms, such as concrete cracking and crushing, steel yielding, as well as interaction phenomena such as steel-concrete slip effects. The 3D model is calibrated and refined through the comparison with experimental data obtained from cyclic tests on real specimens conducted at the University of Basilicata's Laboratory of Structures. The performed analyses aim to improve the procedures for evaluating the seismic behaviour of beam-column joints, facilitating the appropriate design of the SPEAD system. Preliminary numerical analyses have highlighted the beneficial effects of applying the SPEAD device, resulting in an increase in strength and ductility of the beam-column joint, a reduction in steel-concrete slippage phenomena, and decreased damage to the joint panel, enhancing its repairability after seismic events.

Keywords: Existing Buildings - Seismic Vulnerability - Sustainable Strengthening - RC Beam Column Joint - Low Impact Solutions.

ISSN:2623-3347 Published by Eccomas Proceedia.
Peer-review under responsibility of the organizing committee of COMPDYN 2025.
doi: 10.7712/120125.12684.25622

1 INTRODUCTION

One of the most urgent challenges in Europe is reducing the seismic vulnerability of the existing building stock. In recent years, numerous seismic events have caused significant human and economic losses in countries with high seismic risk, such as Italy [1], Greece, and Turkey. The latter was severely affected by the earthquake on February 6, 2023, which caused over 51,000 fatalities, the collapse of 210,000 buildings, and damage to about 890,000 structures [2]. As reported by Masi in [3], in Italy, more than 55% of existing reinforced concrete buildings were constructed without any seismic regulations, as they were built before 1981, the year the D.M. 02/07/1981 came into force.

Furthermore, the construction sector, and particularly the existing structural heritage, is one of the most energy-consuming, with significant environmental impacts [4]. From a sustainable development perspective, it is essential to develop integrated intervention techniques that simultaneously reduce seismic vulnerability and improve the environmental efficiency of buildings [5-7].

Passoni et al. [8] highlight the importance of researching sustainable solutions for the existing building stock, proposing an innovative framework based on the Life Cycle Thinking (LCT) approach for the holistic design of sustainable retrofit interventions. Within the structural strengthening techniques that offer benefits both in terms of seismic and environmental improvements, a central role is played by local strengthening interventions on the beam-column joints of reinforced concrete structures. These interventions improve the capacity of beam-column joints with minimal impact on the building, working mostly from the outside and allowing the building to remain functional during strengthening works.

In addition, the use of innovative techniques and materials promote the decarbonisation of existing buildings. In response to these needs, the scientific community has developed numerous local strengthening techniques characterised by optimal effectiveness and low invasiveness.

In Santarsiero and Masi [9-10] a simple local strengthening system for reinforced concrete joints was proposed. It uses steel L-shaped profiles at the corners of structural elements, wrapped in stainless steel strips, and connected to the beam-column intersection with steel dissipative elements. This system has been effective in increasing the joint's capacity and energy dissipation, but it needs further design refinement. In Frascadore et al.[11] various types of local FRP reinforcements were proposed for the beam-column joints of six reinforced concrete (RC) school buildings in L'Aquila. The results show that this technique can achieve a seismic safety level of approximately 60% of that required for a new building.

In Chung-Chan Hung et al.[12], an innovative retrofit technology is proposed that uses high-strength steel bars and Engineering Cementitious Composite (ECC), a fiber-reinforced material with high tensile strength and damage tolerance. The method aims to reduce the size of the retrofit intervention on the beam-column joint by combining ECC layers with high-strength steel bars. Karayannis and Golias [13] used external carbon fiber ropes to reinforce reinforced concrete beam-column joints, testing eight full-scale subgroups under increasing cyclic deformations. The results showed that the reinforced joints had better hysteretic response, higher maximum loads, greater stiffness and energy dissipation, and less damage compared to the unreinforced joints.

In the work of Molod et al.[14], a superelastic shape memory alloy (SMA) plate is used as an innovative element to strengthen existing reinforced concrete beam-column joints. The authors highlight the sustainability of this technique, noting its quick and low-impact application. However, they also mention the high cost of special alloys, which could limit its use. The examples above show how technological innovations and new materials are becoming more and

more important in strengthening reinforced concrete structures through local interventions. However, many studies have been based on simplified models, without floors and transverse beams. The techniques mentioned may face challenges when demolition of non-structural components, like infill walls, is needed. Some studies focus on exterior-only strengthening solutions to reduce structural impact, but they often have high costs due to innovative materials. Therefore, the aim of this study is to develop a cost-effective, sustainable local reinforcement method for reinforced concrete structures that improves seismic performance and minimizes impact on the structure.

The proposed technique, named Steel Plate Energy Absorption Device (SPEAD)[15], involves a purposely shaped steel plate externally glued to reinforced concrete beam-column joints also using chemical bolts. It is designed to provide a predefined threshold force, activated by the relative deformation between the beam and column, improving seismic capacity and preventing brittle shear failure. The system also shifts the hinge region of the beam, increasing resistance at the beam-column joint. A nonlinear 3D finite element model, calibrated through experimental data from cyclic tests conducted on specimens at the Laboratory of Structures at the University of Basilicata, was employed to evaluate the seismic behaviour of beam-column joints both before and after the intervention. Preliminary analyses indicate that the SPEAD device significantly improves strength, reduces slippage between steel and concrete, and minimizes damage to the joint panel.

2 SPEAD STRENGTHENING SYSTEM

The RC joints beam-column are among the most vulnerable elements in framed structures, as they are subjected to cyclic stresses due to the seismic action, which cause high shear forces and bond-slip phenomena of reinforcement bars (Figure 1). The main issues found in the joints of existing structures are due to the lack of adequate construction details. In particular, the most common defects include: the interruption of the longitudinal reinforcement bars of the beam within the joint panel, the complete absence or insufficient amount of stirrups, which are inadequate to prevent shear failure of the joint and cause a lack of concrete confinement.

Figure 1: Damaged RC beam- column joints with diagonal cracks following an earthquake [16]

This work presents the SPEAD strengthening system [15]. The device is designed to improve the local seismic performance while meeting sustainability criteria. Its external application reduces impact on the structure and uses fewer materials, making it both environmentally and socially sustainable. The device is represented by a steel plate designed to shift the position of the beam plastic hinge, moving it away from the intersection with the column, while simultaneously increasing the seismic capacity of the joint. It consists of two parts: the first is fixed to the column, while the second is fixed to the beam. economically beneficial. The

SPEAD device is installed using chemical anchors (Figure 2), which allow it to be perfectly attached to both the beam and the column. The two parts are bonded at the contact points between the beam and the column using epoxy resin. Before installation, any degraded concrete areas must be repaired to create a smooth and uniform surface on which the steel plate can be properly positioned.

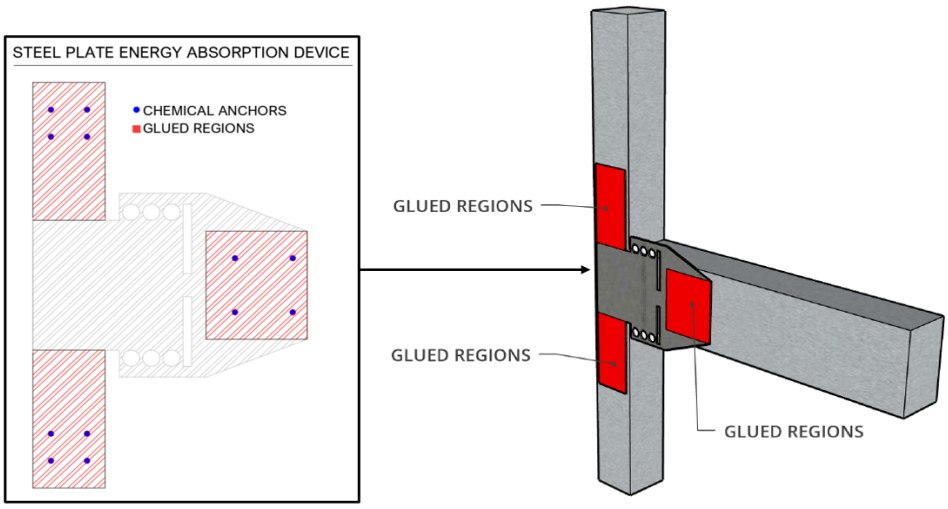

Figure 2: Application of the SPEAD device to RC beam-column joints

The SPEAD system operates through the relative deformations between the beam and the column that occur during seismic events. The plate is designed with circular holes, and hourglass shapes form between consecutive holes that deform under shear stress. This deformation provides a fixed limit force and a dissipation capacity, exploiting the hysteretic behaviour of steel. The forces acting on the device include the horizontal force F_p applied to the lever arm B, the moment M_p, and the shear force V_p that develops along the interface between parts 1 and 2 of the device (Figure 3). This system increases the beam's flexural strength by shifting the plastic hinge to the end of the device (on the right side of part 2). The flexural response of the device is primarily determined by the internal lever arm B', where the centroid of the applied forces F_p is located (Figure 3).

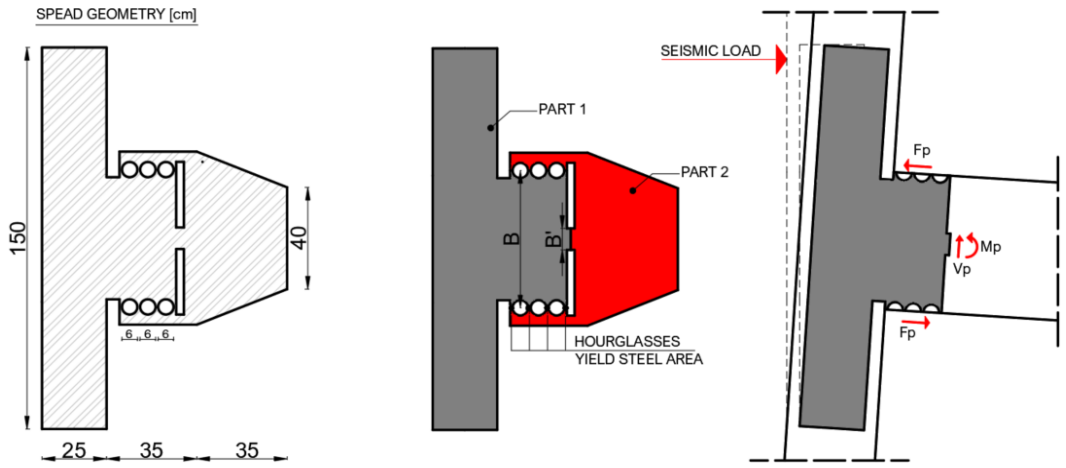

Figure 3: Geometry and functioning of the SPEAD Device

The strengthening system is ideal for beam-column connections where the beam is not much stronger than the column.

To meet capacity design principles, the designer should assess whether the upper and lower columns need additional strengthening, possibly combined with SPEAD components applied to the column. Additionally, it is important to consider that the new location of the plastic hinge of the beam may not have the necessary details to prevent rebar failure and provide adequate concrete confinement.

3 EXPERIMENTAL TESTS ON RC BEAM-COLUMN JOINTS

An experimental campaign was conducted on 26 reinforced concrete beam-column joints At the Structural Laboratory of the University of Basilicata [17]. The aim of the experiment was to analyse how geometric and mechanical parameters, along with different reinforcement configurations and various levels of seismic design, influence the structural behaviour of the joints and their collapse mechanism under seismic loading. Specifically, for this work, the beam-column joint called T4 was analysed, designed according to the Italian standard OPCM 2003[18], and classified as seismic with a Z4 (lowest seismic hazard out of 4 seismic zones) design, corresponding to a low seismicity zone.

The joint consists of the intersection of a column with a 300x300 mm cross section and a beam with a 300x500 mm cross section. The reinforcements are symmetrically distributed both in the column and in the beam. In the column, three longitudinal bars are provided on each side, each with a diameter of 14 mm. In the beam, the reinforcement is symmetric both in the upper and lower parts, with a total of 8 longitudinal bars distributed along the entire element, 2 Ø14 and 2 Ø12 on each side (Figure 4).

Regarding the mechanical properties of the materials, concrete with a compressive strength of f_c = 21.5 N/mm² was used, while B450C class steel bars with improved adherence were chosen, with a yield strength value of $F_{y,\,med}$ = 480 N/mm². These values were derived from laboratory experimental tests.

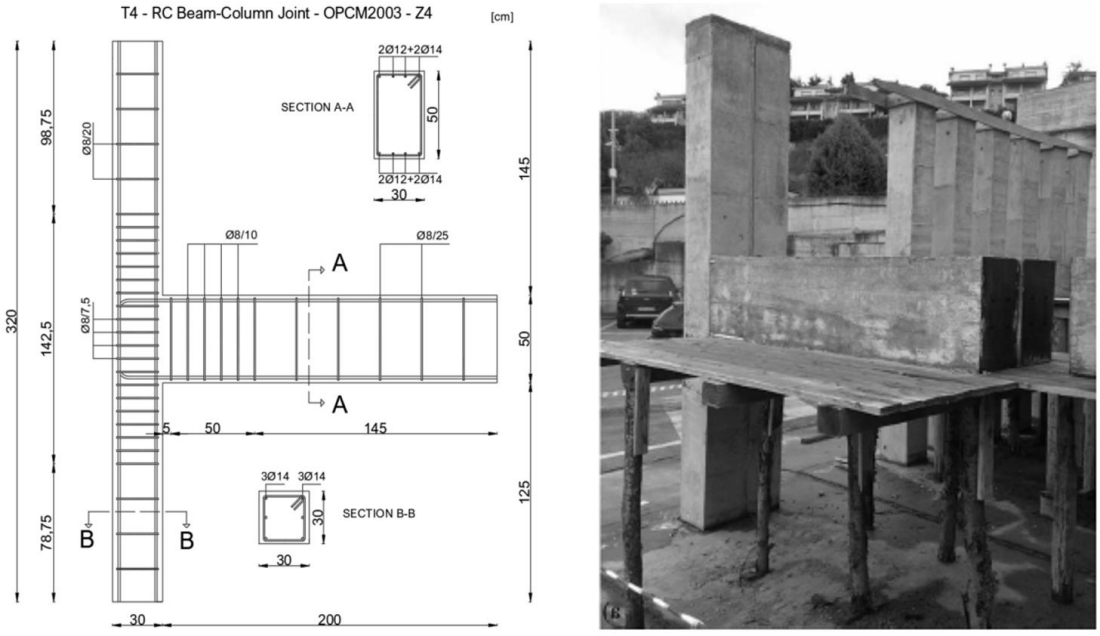

Figure 4: Geometry and design of RC Beam-Column Joints T4

The specimens were subjected to a quasi-static cyclic test with controlled displacement, by applying a horizontal force at the top of the column and an axial force along its axis. The axial force was applied in such a way as to remain parallel to the column's axis, even in the case of rotation, to eliminate the P-Δ effects. An axial force of 580 kN was applied to the T4 specimen.

The testing program was carried out with three cycles for each drift amplitude, with values increasing until a state of severe damage or the near-collapse condition was reached. The full loading scheme (Figure 5) and its history are detailed in the paper [17].

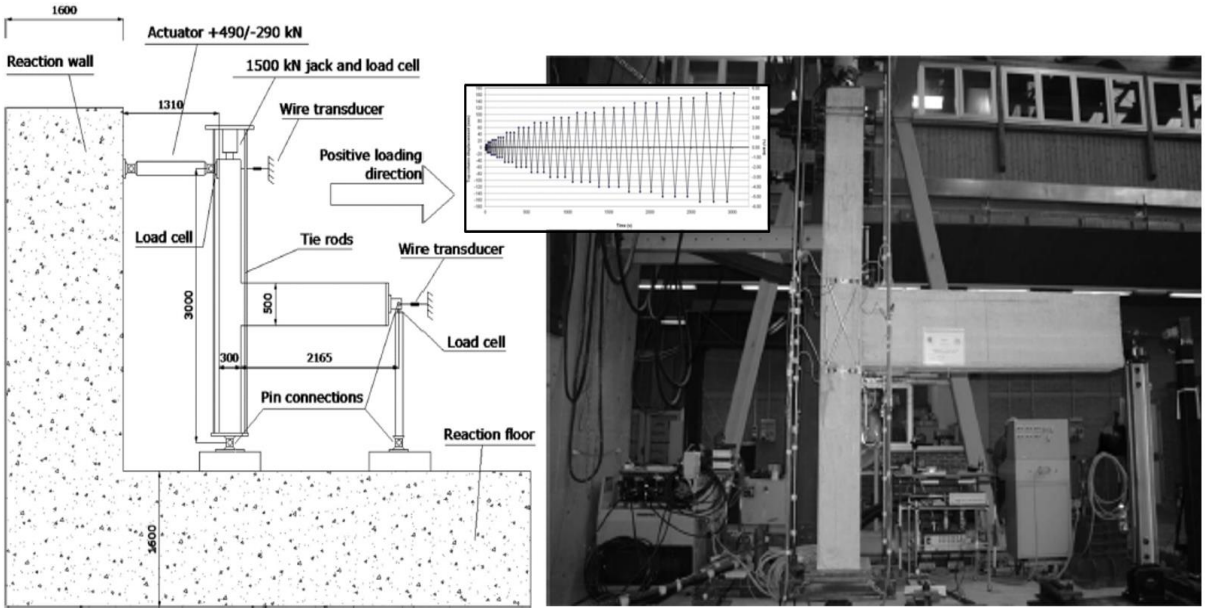

Figure 5: Cycle load test scheme on RC beam - columns joints specimens [17]

4 NUMERICAL MODELLING

After completing the experimental tests, a finite element model (Figure 7) was developed using the ATENA 3D software (version 5.4.1). The first phase consisted of constructing the geometry of the T4 joint, using three-dimensional volumetric elements for the concrete components and one-dimensional elements to model the reinforcement bars. Subsequently, the materials and loads were introduced.

For the materials, the considered mechanical properties were determined based on the results from the previously mentioned tests conducted on several specimens during the experimental phase, resulting in an average cylindrical compressive strength value of f_c=21.5 N/mm^2. Using this value, all other concrete properties were derived in accordance with NTC18 [19] and Eurocode 2 [20]. The derived values are listed in figure 7.

The developed model is nonlinear, with the formulation of the constitutive relations considered in the plane stress state. To represent the damage of the concrete, a smeared crack approach was adopted. The nonlinear behaviour of the material under biaxial stress conditions is described using the effective stress and the equivalent uniaxial strain, the latter introduced to eliminate the Poisson effect in the plane stress state.

The behaviour of concrete under tensile stress is initially linear until the max strength is reached. Once this strength is surpassed, a fictitious crack model is employed, based on an exponential crack-opening law and fracture energy, to simulate crack propagation [21]. The adopted constitutive laws are shown in the Figure 6. In the smeared crack approach, fracture energy G_F is essential for the model accuracy.

Without direct experimental data for the concrete used, fracture energy was determined using the expression from the CEB-FIP 2010 model code [22]:

$$G_F = 73(f_c)^{0.18} \quad \text{Fracture Energy} \quad (1)$$

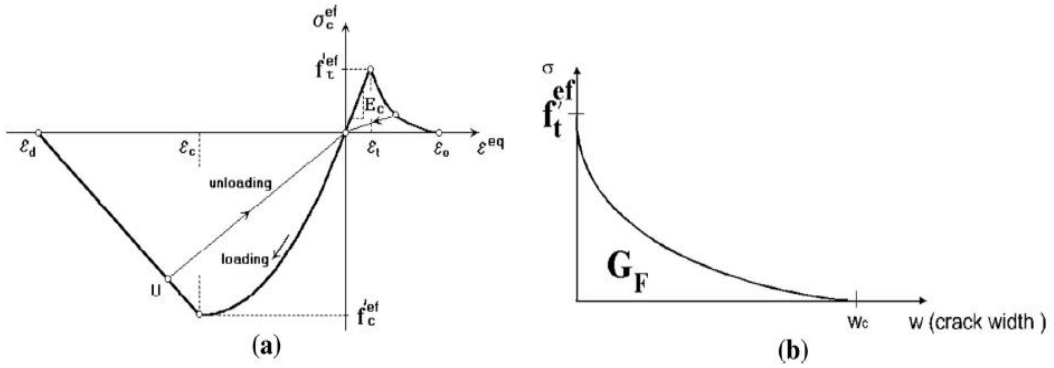

Figure 6: Complete uniaxial stress–strain law (a) and exponential crack opening law in tension (b) for concrete [21]

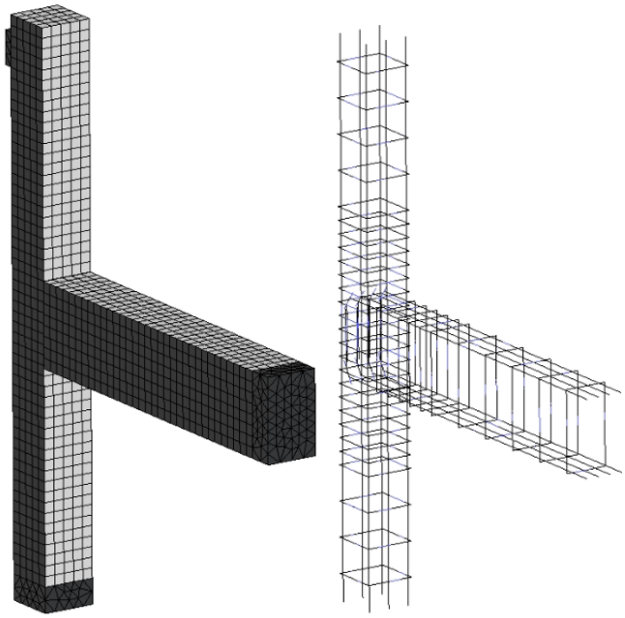

CC3DNonLinCimentitious2 - Concrete model parameters

Parameter	*Units*	*Value*
Uniaxial Compressive Strength f_c	*N/mm²*	21.5
Elastic Modulus E	*N/mm²*	27679.24
Tensile strenght f_t	*N/mm²*	2.0
Unit fracture Energy U	*N/mm*	0.127
Coefficient Poisson	---	0.2

CCReinforcement - Reinforcement model parameters

Parameter	*Units*	*Value*
Yield Strength of Steel F_{yk}	*N/mm²*	480
Steel Elastic Modulus Es	*N/mm²*	200 000
Ultimate Strength of Steel F_{yu}	*N/mm²*	590
Ultimate strain ε_u	---	0.12

Finite Element Mesh

Elements	*Mesh Type*	*Nodes*
Concrete	*Hexahedral*	2645
Reinforcements	*Linear*	173
Steel Bearing Plate	*Tetrahedral*	1710

Figure 7**:** Finite element model of the RC beam-column joint and related mechanical parameters

For the reinforcement, both for the longitudinal bars and the stirrups, steel class B450C was used, as specified by the Italian structural code [19], corresponding to hot-rolled steel class C according to Eurocode 2 [20]**.** Tensile tests, in the experimental phase, were conducted on the steel bars which reached an average yield strength 480 N/mm² and an ultimate strength of 590 N/mm², with a strain of 12%.

Based on the experimental results, an elastoplastic constitutive law with strain hardening was implemented in the numerical model. Finally, ATENA can apply the bond-slip law for

reinforced concrete in the numerical model. Used the model from the CEB-FIP Model Code 2010 (Figure 8).

The parameters considered include the type of failure mode, which is of the Splitting type, as well as the condition of the concrete. The specimens are assumed having good quality bond conditions. Additionally, the presence or absence of confinement is considered; in this case, stirrups are present. Based on these factors, we can calculate the maximum shear stress $\tau_{max} = 8\,(f_c/25)^{0.25} = 7.70$ N/mm^2 [22].

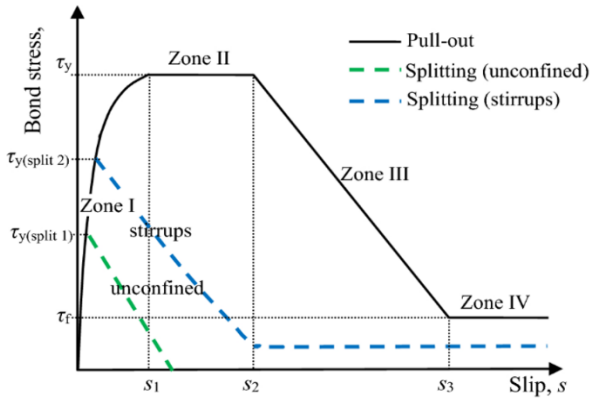

	1	2	3	4	5	6
	Pull-Out (PO)		Splitting (SP)			
	$\varepsilon_s < \varepsilon_{s,y}$		$\varepsilon_s < \varepsilon_{s,y}$			
	Good bond cond.	All other bond cond.	Good bond cond.		All other bond cond.	
			unconfined	stirrups	unconfined	stirrups
τ_{bmax}	$2.5\sqrt{f_{cm}}$	$1.25\sqrt{f_{cm}}$	$7.0\cdot\left(\frac{f_{cm}}{25}\right)^{0.25}$	$8.0\cdot\left(\frac{f_{cm}}{25}\right)^{0.25}$	$5.0\cdot\left(\frac{f_{cm}}{25}\right)^{0.25}$	$5.5\cdot\left(\frac{f_{cm}}{25}\right)^{0.25}$
s_1	1.0 mm	1.8 mm	$s(\tau_{bmax})$	$s(\tau_{bmax})$	$s(\tau_{bmax})$	$s(\tau_{bmax})$
s_2	2.0 mm	3.6 mm	s_1	s_1	s_1	s_1
s_3	c_{clear} [1)]	c_{clear} [1)]	$1.2s_1$	$0.5c_{clear}$ [1)]	$1.2s_1$	$0.5c_{clear}$ [1)]
α	0.4	0.4	0.4	0.4	0.4	0.4
τ_{bf}	$0.40\,\tau_{bmax}$	$0.40\,\tau_{bmax}$	0	$0.4\,\tau_{bmax}$	0	$0.4\,\tau_{bmax}$

1) c_{clear} is the clear distance between ribs

Figure 8: Bond model (CEB-FIP model code 2010)[22]

Once the mechanical parameters were obtained, a finite element mesh was defined for the numerical model. For the concrete, a structured mesh of 8-node hexahedral elements was used, while for the reinforcement bars, a linear mesh was employed, capable of absorbing only axial loads.

In total, the model consists of 4,441 nodes, divided into 173 linear elements, 2,645 hexahedral elements, and 1,710 tetrahedral elements, the latter used for the steel bearing plates. The discretization of the hexahedral elements was carefully carried out through a sensitivity analysis, and the average size of these elements is 0.06 m.

The numerical analysis on the T4 joint was performed by applying a load for surface of 6.45 N/mm² (to simulate the axial load) distributed on the top of the column, along with an incremental horizontal displacement applied monotonically at a height of 3 meters from the base. The analyses were conducted only for positive displacements.

4.1 Comparison of experimental and numerical results

With reference to the parameters used in [17], comparisons were made between the values obtained from the experimental test and those from the numerical model. During the cyclic test, specimen T4 exhibited a flexural-type failure, with cracking primarily affecting the lower part of the beam, which was subjected to tensile stresses.

The cracking of the reinforced concrete occurred at relatively low stress levels, initially arising at the intersection between the column and the beam. This caused the expulsion of concrete cover and led to premature failure (due to low cycles fatigue) due to the instability of the bottom reinforcement of the beam, to a drift value of 3%.

Examining the damaged specimen (Figure 9), it was noted that the concrete cover in the upper part of the beam exceeded the 40 mm specified in the design (actual value between 80-90 mm). This discrepancy, considered in the calibration process, was due to mistakes occurred during the construction phase.

***T4** - Flexural mechanism, cracking in beam element*

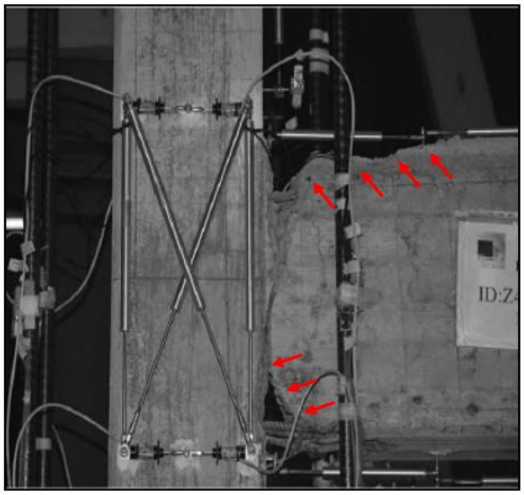

Figure 9: Collapse mechanisms for specimens T4

To calibrate the numerical model and its associated mechanical parameters, the load-drift curve trends were analysed, considering the peak value of the maximum force (F_{max}), the corresponding drift value (d_y), and the ultimate drift (d_u), which is conventionally defined as the value at which a 20% reduction in Fmax is observed.

The peak force value recorded during the experimental test was 42.9 kN, with the post-peak force behaviour remaining stable between 1% and 3% drift. At 3% drift, the lower reinforcement failed due to buckling (d_b = 3%), leading to a significant decrease in strength. The calibration process mainly focused on the parameters influencing the propagation of cracks in the concrete. The optimal match was obtained when the upper reinforcement was shifted 40 mm downwards, effectively replicating the actual 80 mm concrete cover in the upper zone.

***JOINT T4 - Z4 OPCM 2003** - Comparison Experimental Test with Numerical Model*

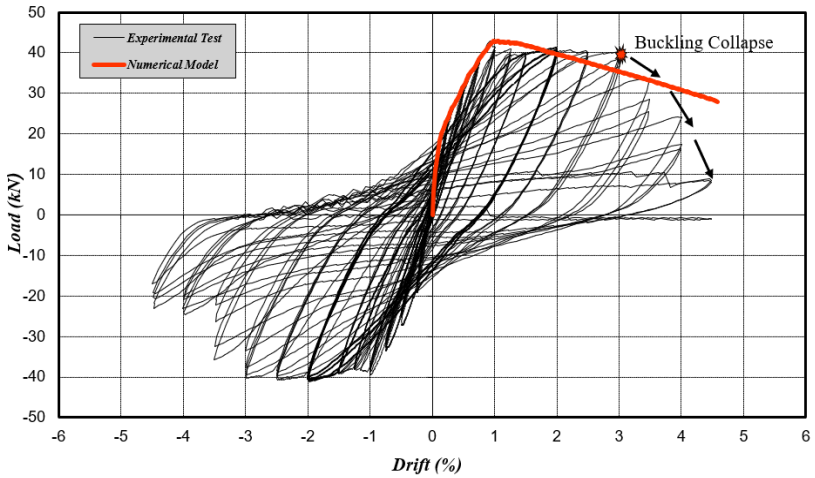

***Faillure Type:** A purely flexural mechanism involving primarily the beam element*

Experimental Test

Parameter	*Units*	*Value*
Fmax	*kN*	42.9
d_y	*%*	0.93
d_u	*%*	3.45

Numerical Model

Parameter	*Units*	*Value*
Fmax	*kN*	42.98
d_y	*%*	0.99
d_u	*%*	3.25

Figure 10: Load-Drift comparison between experimental test and calibrated numerical model, specimen T4

Table 1: presents the percentage variations between the experimental and numerical parameters, with percentage differences not exceeding 7%. It is important to note that the numerical model is unable to replicate the experimental load-drift curve after buckling failure, which occurred at 3% drift (equivalent to a displacement of 100 mm). However, this does not affect the objectives of this study.

Experimental			*Numerical*			*Scatter* Δ		
F_{max} [kN]	d_y [%]	d_u [%]	F_{max} [kN]	d_y [%]	d_u [%]	F_{max} [%]	d_y [%]	d_u [%]
42.9	*0.93*	*3.45*	*42.98*	*0.99*	*3.25*	***+0.19***	***+6.45***	***-5.80***

Table 1: Comparisons of experimental and numerical results

5 THE NUMERICAL APPLICATION OF SPEAD DEVICE

The numerical model showed a good agreement with the experimental data, and for this reason, the SPEAD system was integrated into the finite element nonlinear model. The SPEAD system (Figure 3) consists of circular holes with a diameter of 60 mm, spaced 10 mm apart, corresponding to the thickness of the hourglasses. The number of holes was chosen to ensure enough hourglasses, providing stable hysteretic behaviour, even if one fails under seismic loading. Arm B' was set to 85 mm, a dimension large enough to ensure adequate shear stiffness in the connection between parts 1 and 2, thereby preventing excessive tensile stresses on the hourglasses, which are designed to work primarily under shear forces.

The internal lever arm B was determined using the procedure described in [15], with a calculated value of 540 mm. This value is crucial for determining the yielding moment of the plate M_{yspead}.

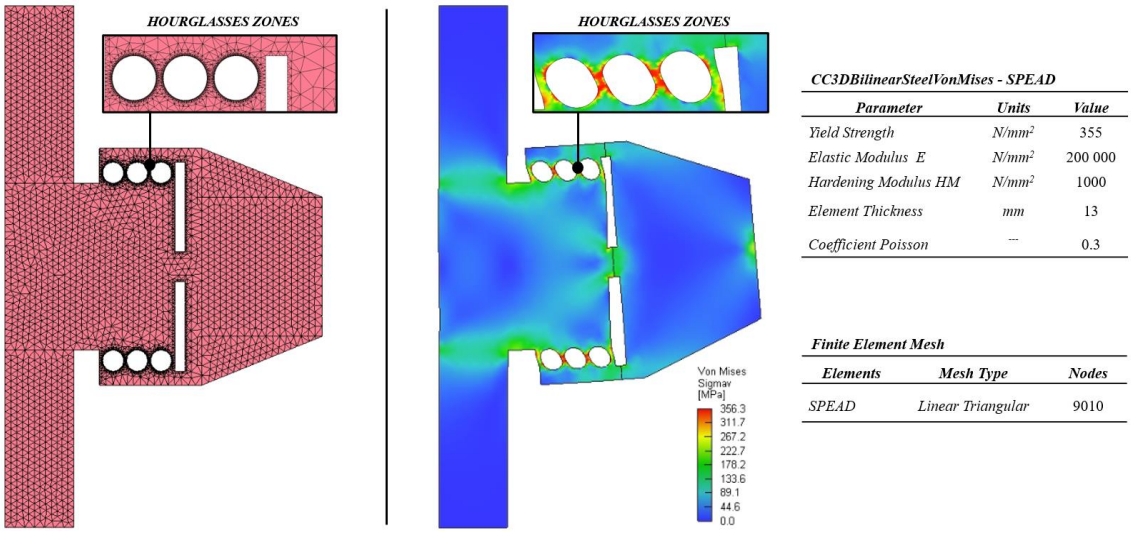

Figure 11: Mesh for SPEAD device with refinement in hourglass regions and related plastic deformation mechanism

The plate was extended along the columns to cover the entire critical zone, with an extension of 500 mm above and below the joint panel. A plate thickness of 13 mm was selected to prevent buckling in the regions of the device that are subjected to compression. Alternatively, this issue could be addressed by adding stiffening ribs welded to the plate.

The material used is S355 steel, as specified by the Italian seismic code, with a characteristic yield stress of f_{yk} = 355 N/mm^2. The constitutive model is elastic–perfectly plastic, with a hardening modulus of 1000 N/mm^2. The device was then modelled in ATENA using 9,010 linear triangular elements, with a refined mesh applied in areas where plasticization is ex-

pected. The mesh size ranges from 0.005 m to 0.02 m, depending on the regions with higher plastic deformations, such as the hourglasses zones (Figure 11).

5.1 Evaluation of the post-intervention seismic performance

The SPEAD system was integrated into the finite element numerical model in such a way as to accurately simulate the installation of the device, as described in Section 2. Perfect boundary conditions were applied at the contact areas between the SPEAD device and the reinforced concrete beam-column joint. Once the strengthening system was integrated, the numerical analysis was carried out in the same way, using the same applied loads, compared to the test conducted in the as-built condition.

Upon completing the analysis, comparisons were made using the same parameters as in the previous analysis, including the Load-Drift curve, maximum peak force (F_{max}), the corresponding yield drift value (d_y), and the ultimate drift value (d_u), defined as the displacement corresponding to a 20% reduction in the maximum force. Based on the results, specimen T4 demonstrates a significant improvement in terms of seismic capacity.

In the T4 joint model with SPEAD, the maximum load (F_{max}) reaches 58.26 kN, with a yield drift of 1.59%. Compared to the data regarding the as-built specimen model, there is a notable improvement, with a 35.55% increase in resistance.

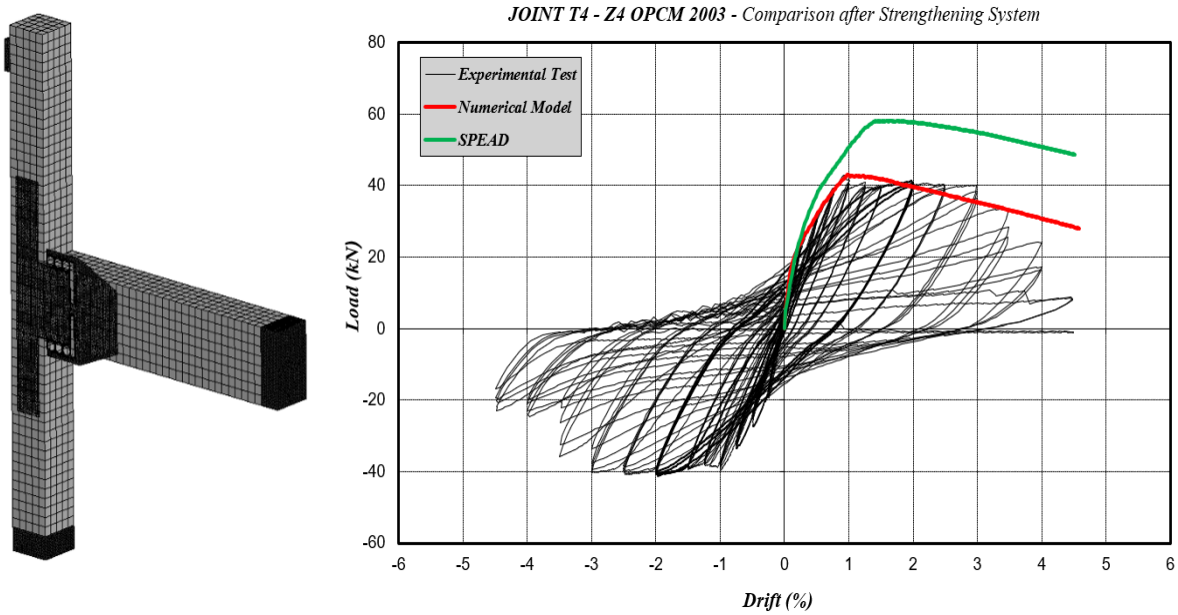

Figure 12: Comparison of Load - Drift curves after the application of the SPEAD device

Furthermore, the yield drift increases by more than 60% compared to the model without SPEAD. Regarding secant stiffness, no significant improvement is observed in the T4 beam-column joint at a drift of 0.5%, which corresponds to the damage limitation state as per the Italian seismic code. The stiffness and ductility of the strengthened numerical model remains nearly identical to that of the unstrengthened model (Figure 12).

Table 2 presents the performance indicators of the numerical model without (As Built) and with SPEAD, and the percentage variations, allowing for a clear comparison of the improvements.

Numerical Model As Built			***Numerical Model with SPEAD***			***Scatter Δ***		
F_{max} *[kN]*	d_y *[%]*	d_u *[%]*	F_{max} *[kN]*	d_y *[%]*	d_u *[%]*	F_{max} *[%]*	d_y *[%]*	d_u *[%]*
42.98	*0.99*	*3.25*	*58.26*	*1.59*	*5.02*	***+35.55***	***+60.6***	***+54.5***

Table 2: Numerical comparison after applying the SPEAD system

6 CONCLUSIONS

The numerical analyses conducted in this study aim to develop a local strengthening technique that combines the reduction of seismic vulnerability of existing buildings with the adoption of sustainable and low-impact solutions. This technique is designed to increase the seismic capacity of reinforced concrete structures while keeping costs low in economic, environmental, and social terms.

The SPEAD (Steel Plate Energy Absorption Device) system is based on the application of a steel plate to the RC beam-column joints, installed on the exterior of the building without interfering with or damaging the slab, infill walls, or transverse beams. This low-impact approach is one of the key aspects of the solution, as it does not compromise the daily life and social activities of the building occupants. The study was based on the creation of a nonlinear finite element numerical model, calibrated on a cyclic experimental test performed on a reinforced concrete beam-column joint, conducted at the laboratories of the University of Basilicata.

The pre- and post-intervention performance evaluated on the numerical model was compared, analysing the differences and improvements in terms of strength, stiffness, and ductility. The results obtained are promising specimen T4 showed a significant increase in terms of resistance, while maintaining similar values in stiffness and ductility.

The SPEAD system increases the bending moment capacity of the beam, in line with the principles of capacity design, and significantly contributes to the reduction of damage both in the joint panel and other structural components.

An additional advantage lies in the translation of the plastic hinge from the beam-column interface to the interface between the beam and the SPEAD device. This results in a reduction of slippage phenomena at the joint or beam-column interface, being more distributed over the beam.

Despite the promising results, the numerical data still represents a preliminary analysis, and further investigations through targeted experimental campaigns are required to more accurately quantify the effects of SPEAD devices on reinforced concrete structures.

Additionally, the application of the device to real buildings would be particularly useful for optimizing the installation process, allowing for a direct assessment of the benefits and any limitations arising from the application of the device only on the exterior of the structure.

REFERENCES

[1] T. Rossetto, N. Peiris, J.E. Alarcon, E. So, S. Sargent, M. Free, V. Sword Daniels, D. Del Re, C. Libberton, E. Verrucci, et. al., Field observations from the Aquila, Italy earthquake of April 6, 2009. *Bulletin of Earthquake Engineering,* 9, 11-37, 2011.

[2] L. Dal Zilio, J.P. Ampuero, Earthquake doublet in Turkey and Syria. *Communications Earth & Environment*, 4(1), 71, 2023.

[3] A. Masi, Seismic Vulnerability Assessment of Gravity Load Designed R/C Frames. *Bulletin of Earthquake Engineering* 1, 371–395, 2003.

[4] A. Marini, C. Passoni, P. Riva, P. Negro, E. Romano, F. Taucer, *Technology options for earthquake resistant, eco-efficient buildings in Europe: Research needs. European commission, joint research centre scientific and policy reports,* 2014.

[5] G. Santarsiero, A. D'Angola, G. Ventura, A. Masi, V. Manfredi, V. Picciano, A. Digrisolo, Sustainable Renovation of Public Buildings through Seismic–Energy Upgrading: Methodology and Application to an RC School Building. *Infrastructures,* 8(12), 168, 2023.

[6] V. Manfredi, A. Masi, Seismic strengthening and energy efficiency: Towards an integrated approach for the rehabilitation of existing RC buildings. *Buildings,* 8(3), 36, 2018.

[7] G. Santarsiero, M. Misceo, P. Aversa, E. Candigliota, A. Di Micco, F. Hugony, V. Manfredi, G. Marghella, A. Marzo, A. Masi, et.al., Holistic Assessment for Social Housing Retrofitting: Integrating Seismic, Energy, and Social Aspects in the REHOUSE Project. *Buildings*, 14, 3659, 2024.

[8] C. Passoni, A. Marini, A. Belleri, C. Menna, Redefining the concept of sustainable renovation of buildings: State of the art and an LCT-based design framework. *Sustainable Cities and Society,* 64, 102519, 2021.

[9] G. Santarsiero, A. Masi, Seismic performance of RC beam–column joints retrofitted with steel dissipation jackets. *Engineering Structures*, 85, 95-106, 2015.

[10] G. Santarsiero, A. Masi, Seismic Upgrading of RC Wide Beam–Column Joints Using Steel Jackets. *Buildings*, 10, 203, 2020.

[11] R. Frascadore, M. Di Ludovico, A. Prota, G. M Verderame, G. Manfredi, M. Dolce, E. Cosenza, Local strengthening of reinforced concrete structures as a strategy for seismic risk mitigation at regional scale. *Earthquake Spectra*, 31(2), 1083-1102, 2015.

[12] C. C. Hung, H. J. Hsiao, Y. Shao, C. H. Yen, A comparative study on the seismic performance of RC beam-column joints retrofitted by ECC, FRP, and concrete jacketing methods. *Journal of Building Engineering,* 64, 105691, 2023

[13] C. G. Karayannis, E. Golias, Full-scale experimental testing of RC beam-column joints strengthened using CFRP ropes as external reinforcement. *Engineering Structures*, 250, 113305, 2022.

[14] M. A. Molod, F. J. Barthold, P. Spyridis, Minimally Invasive Retrofitting of RC Joints with Externally Applied SMA Plate—Adaptive Design Optimisation through Probabilistic Damage Simulation. *Sustainability*, 15(4), 3831, 2023.

[15] G. Santarsiero, V. Manfredi, A. Masi, Numerical evaluation of the steel plate energy absorption device (SPEAD) for seismic strengthening of RC frame structures. *International Journal of Civil Engineering*, 18(8), 835-850, 2020.

[16] M. Dolce e G. Manfredi, Guidelines for repair and strengthening of structural elements, infills and partitions. *RELUIS*, 2011.

[17] A. Masi, G. Santarsiero, D. Nigro, Cyclic Tests on External RC Beam-Column Joints: Role of Seismic Design Level and Axial Load Value on the Ultimate Capacity. *Journal of Earthquake Engineering*, 17(1), 110–136, 2012.

[18] Ordinance of the President of the Council of Ministers (OPCM) 20 March 2003, n.3274, ‘‘Primi elementi in materia di criteri generali per la classificazione sismica del territorio nazionale e di normative tecniche per le costruzioni in zona sismica’’. Official Journal, General serie n.105, 08-05-2003 – Ordinary Supplement n. 72 (in Italian). www.gazzettaufficiale.it

[19] MinistryDecree 17 gennaio 2018, ‘‘Aggiornamento delle «Norme tecniche per le costruzioni»’’, Official Journal, General serie n.42, 20-02-2018—Ordinary Supplement n. 8 (in Italian). www.gazzettaufficiale.it

[20] CEN (2004). EN 1998-1:2004 Eurocode 2—design of concrete structures—part 1: general rules and rules for buildings

[21] Cervenka Consulting (2000–2014) ATENA program documentation, part 1, ATENA Theory Manual

[22] MC10 (2010) CEB-FIP Model Code 2010. Comite´ Euro-International duBe´ton